Total and positronium formation cross sections for positron scattering from H_2O and HCOOH

2009 New J. Phys. 11 103036

(http://iopscience.iop.org/1367-2630/11/10/103036)

New Journal of Physics
The open-access journal for physics

Total and positronium formation cross sections for positron scattering from H_2O and HCOOH

Casten Makochekanwa[1,5], Ana Bankovic[2], Wade Tattersall[1,3], Adric Jones[1], Peter Caradonna[1], Daniel S Slaughter[1], Kate Nixon[4], Michael J Brunger[4], Zoran Petrovic[2], James P Sullivan[1] and Stephen J Buckman[1]

[1] ARC Centre for Antimatter-Matter Studies, Research School of Physics and Engineering, Australian National University, Canberra, ACT 0200, Australia
[2] Institute of Physics Belgrade, University of Belgrade, Pregrevica 118, POB 68, 11080 Zemun, Serbia
[3] ARC Centre for Antimatter-Matter Studies, James Cook University, Townsville 4810, Australia
[4] ARC Centre for Antimatter-Matter Studies, School of Chemistry, Physics and Earth Sciences, Flinders University, GPO Box 2100, Adelaide, SA 5001, Australia
E-mail: cxm107@physics.anu.edu.au (C Makochekanwa)

New Journal of Physics **11** (2009) 103036 (22pp)
Received 12 August 2009
Published 21 October 2009
Online at http://www.njp.org/
doi:10.1088/1367-2630/11/10/103036

Abstract. Total and positronium formation cross sections have been measured for positron scattering from H_2O and HCOOH using a positron beam with an energy resolution of 60 meV (full-width at half-maximum (FWHM)). The energy range covered is 0.5–60 eV, including an investigation of the behavior of the onset of the positronium formation channel using measurements with a 50 meV energy step, the result of which shows no evidence of any channel coupling effects or scattering resonances for either molecule.

[5] Author to whom any correspondence should be addressed.

Contents

1. Introduction

The importance of ionizing radiation in biological molecules has become an area of intense interest of late. The most significant observation is that most of the energy deposited in cells by ionizing radiation is channeled into the production of free secondary electrons with energies below typically 20 eV. In addition, it has also been demonstrated that the subsequent reactions of such electrons, even at energies well below ionization thresholds, induce substantial yields of single- and double-strand breaks in DNA, through the process of dissociative electron attachment [1]. Positrons have also been recently highlighted [2] as a possible agent in the treatment of tumors—positherapy— and while there may be some similarities in the interaction mechanisms for positrons and electrons with molecules in the body, there are also many differences.

Water (H_2O) is present in the atmospheres of most planets of the solar system, as well as the Sun itself. It is also the third most abundant molecule in the Universe (after H_2 and CO) [3] and is regarded as the most important greenhouse gas in the terrestrial atmosphere [4], in the standard thermal balance of the atmosphere. It makes up the main constituent of all living organisms and provides the medium for most chemical and biochemical processes that take place therein [5]. Formic acid (HCOOH) is the simplest organic acid, and is thought to play a major role in the formation of some larger biomolecules such as glycine and acetic acid. In addition, the derivative formate group (–COOH) is a key component of more complex biomolecules including some of the amino acids and DNA bases [6].

The most notable use of positrons in the human context, however, is in positron emission tomography (PET) scans. This essentially non-invasive, medical diagnostic tool has become widely utilized in most major hospitals as an early detection mechanism for tumors, and a general diagnostic of metabolic activity. PET scans involve the release of a high-energy positron into the body, and the detection of the resultant gamma rays which arise upon annihilation with an electron. The processes that occur between the emission of the high-energy particle and the production of gamma rays, involve positron–molecule scattering, but as yet there is essentially no fundamental, quantitative knowledge of these interactions. For example, an understanding of the atomic and molecular processes that take place when a positron interacts with water or the DNA base molecules would be invaluable [7, 8]. A knowledge of both integral and angular differential cross-sections underpins the understanding of the microscopic distribution of energy deposition which is needed for accurate dosimetry (see for example [9]). Furthermore, studies

of positronium (Ps) formation, a critical reaction channel for PET, are likely to be critical in the development of such a dosimetry.

Following the important establishment of the effect of ionizing radiation to biological molecules reported by Boudaiffa *et al* [1] in 2000, much experimental and theoretical activity has become focused on electron scattering from biomolecules, including H_2O and HCOOH. The work on H_2O has been well summarized in the review article by Itikawa and Mason [5], while the recent work on HCOOH is addressed by Zecca *et al* [6] and references therein. While a considerable data library is now available for positron scattering from many atoms and molecules using moderate energy resolutions of a few hundred meV [10], data on positron scattering from H_2O and HCOOH remain scarce and fragmentary, and mainly for grand total cross sections (GTCS).

Previous literature reports for experimental positron scattering from H_2O are from the Yamaguchi group [11]–[13], who used a magnetically guided beam in a time-of-flight apparatus to measure GTCS over the energy range 1–400 eV, and the Trento group [14] who used an electrostatic and magnetic field experimental apparatus to measure GTCS over the energy range 0.1–20 eV. The group at University College London used a magnetically guided beam to measure GTCS (7–417 eV) [15] and Ps formation (10–100 eV) cross sections [16], and an electrostatic apparatus to study the energy distributions of positrons scattered at 0° from these molecules in coincidence with the remnant ions (H_2O^+, OH^+ and H^+) at 100 and 153 eV incident energies [17]. As for the experimental literature on HCOOH, once again the only data are from the Yamaguchi [13] and Trento [6] groups, who both investigated GTCS over the energy ranges 0.7–600 and 0.3–50.2 eV, respectively. Theoretically, we are only aware of a few reports on positron–H_2O scattering, involving computations of positron annihilation rates, Ps formation, and elastic differential and integral cross sections. See for example Hervieux *et al* [18] and Baluja *et al* [19], and references therein. For positron–HCOOH, we are not aware of any other theoretical work besides the use of the Schwinger multichannel method to calculate elastic integral cross sections—jointly published with the experimental GTCS in [6].

In this paper, we report measurements of 0.5–60 eV GTCS and Ps formation cross sections (Q_{Ps}) for positron scattering from H_2O and HCOOH. These measurements were carried out at the Australian Positron Beamline Facility [20], using an energy resolution of ∼60 meV. Because of this superior energy resolution, we have also carried out high precision measurements to investigate threshold effects in the Ps formation and ionization channels, as well as a search for positron scattering resonances.

2. Experimental procedure

The experimental apparatus used for these measurements is based on the Surko trap system, developed at UCSD [21, 22], and has been comprehensively described elsewhere [20]. Only a brief overview of the operation will be presented here. Positrons are obtained from a radioactive source of ^{22}Na, which had an activity of ∼25 mCi for the measurements in this paper. A neon moderator is used to form a low energy positron beam with a measured energy width of ∼1.5 eV. The moderated beam of positrons is confined radially using solenoidal magnetic fields and sent into a three-stage buffer-gas trap. The trap electrodes form a stepped electrostatic potential well, and positrons lose energy inside the trap through inelastic collisions with a mixture of N_2 and CF_4 buffer gases. They are thus confined in the trap where they continue to collide with the gas until they thermalize to the gas (room) temperature. This trapped cloud of positrons becomes

the reservoir for a pulsed positron beam. Trap operation is typically cycled at approximately 100–200 Hz with up to 1000 positrons per pulse. Careful control over the beam formation means that the energy width of the beam is comparable to the temperature of the trapped positron cloud. In these experiments, the typical energy resolution was 60 meV.

The positron beam is directed to a gas cell of length 200 mm and made of gold-plated copper, which contains the target H_2O or HCOOH gas. The gas cell entrance and exit apertures are 5 mm in diameter. The potential of the gas cell defines the energy of the positrons within the cell and the target gas is localized to the 200 mm path length. Target density inside the cell is maintained such that the total positron scattering is less than or equal to 10% of the unscattered beam, in order to avoid multiple scattering effects. The beam transmitted through the gas cell passes through a retarding potential analyzer (sensitive only to the parallel energy component of the beam or $E_\parallel$) and then on to a double-stack, micro-channel plate detector. The collected current is measured and the data stored by the experimental control computer. In a collision with a target gas molecule, the positron can be scattered through some angle θ, losing $E_\parallel$, and it can also lose some of its total energy if inelastic processes are energetically allowed [23]. Ps formation is also possible above the Ps formation threshold, E_{Ps}, corresponding to 5.821 eV for H_2O and 4.53 eV for HCOOH. For the measurements presented in this paper, the incident current (I_0), the total transmitted current (I_{T}) and the transmitted current that had lost any portion of parallel energy (I_{m}) were measured. These cross sections (σ) are derived using the Beer–Lambert attenuation law, namely:

$$Q = -\frac{1}{n\ell}\ln(R), \tag{1}$$

where n is the gas number density, ℓ is the path length through the target gas and R is the appropriate ratio, as defined below. The ratio I_{T}/I_0 gives the Q_{Ps}, I_{m}/I_0 gives the GTCS and $I_{\mathrm{m}}/I_{\mathrm{T}}$ gives the GTCS without Ps formation, i.e. hereafter abbreviated as GTCS $- Q_{\mathrm{Ps}}$. l was taken as the geometrical length of the scattering cell. It was experimentally established to be so, as long as the total scattering probability inside the cell is kept less than 10%, by measurement of the benchmark total cross sections for He [20, 24].

High-purity H_2O and HCOOH were used throughout each study. In addition, since the samples come in liquid form, each liquid was degassed with a freeze, pump and thaw procedure. However, at room temperature, HCOOH presents some challenges to the experimentalist as the sample will consists of both its dimer and monomer forms, with the degree of dimerization depending on the pressure and temperature of the HCOOH sample used [25]. Following the equations derived by Waring [26], from the experimental results of Coolidge [25], the percentage dimer target composition as a function of sample pressure, for our cell temperature of 30.4 °C, was calculated to be about 0.05% for the highest pressure used in the current measurements (0.2 mTorr). Therefore dimer effects in the present cross sections measurements will be negligible.

It is essential in these types of studies that the energy scale is calibrated accurately. In our experimental technique, the zero for the energy scale is established in the absence of the target gas and was determined here with a retarding potential analysis of the beam, i.e. with the energy scale defined relative to the cut-off position of the beam. The accuracy in this measurement gives an error of ∼10 meV in our energy scale. It is also crucial to accurately measure the scattering cell target pressure. The pressure gauge used is a high accuracy Model 690 MKS Baratron capacitance manometer with a full range of 1 Torr and a measurement accuracy of ±0.05%. The gauge is regulated to operate at 45 °C, while the scattering cell is at a temperature

Table 1. Approximate missing angular ranges, 0°–$\theta^\circ_{\max}$, for selected positron scattering energies.

Energy (eV)	$\theta^\circ_{\max}$
0.5	33
1.0	23
2.5	16
5.0	10
15.0	6
30.0	4
60.0	3

of ∼30.4 °C. Since the scattering cell temperature was different from the gauge temperature, a thermal transpiration correction has been applied to the pressure readings. This correction has been calculated according to the model of Takaishi and Sensui [27], and is ∼2.3% for both H_2O and HCOOH over the entire energy range of measurements. The molecular diameter used in this correction was 4.60 Å [28] and 3.8 Å [29] for H_2O and HCOOH, respectively. As already highlighted above, our knowledge of positron scattering from both H_2O and HCOOH is rather scant. What we know from the literature is that both molecules are highly polar and have large dipole polarizabilities, i.e. 1.85 D and ∼10 a.u. for H_2O and 1.41 D and 22.5 a.u. for HCOOH [30]. As such, the elastic differential scattering cross sections (DCS) for both molecules are expected to be dominated by the long-range dipole interaction effects, resulting in highly forward peaked cross sections at lower positron impact energies, i.e. typically below 10 eV. Because of the inevitable angular resolution limitation in our experimental technique, this poses the problem that the cross sections we present here will likely be an underestimation of the actual values for energies below a few eV, depending on the nature of the elastic DCS for each molecule. Our technique relies on measuring the transmitted positron current (I_m) at the beam cut-off point on the retarding potential analyzer voltage axis (see [23] for full details on this technique). In practice, however, it is not possible to make a measurement of the quantity I_m at exactly the cut-off voltage, as this coincides with the cut-off point of the unscattered positron beam. To avoid effects associated with the cut-off, the positron current must be measured at a retarding potential voltage sufficiently offset from the cut-off. This was done for measurements of both gases at $\delta E = 150$ meV (i.e. more than three standard deviations) away from the cut-off, or at $E - \delta E$, where E is the beam energy. This restriction means that the measured total cross section excludes some contribution from DCS corresponding to this inaccessible δE range. Using the equations discussed in [23], the missing angular range, 0°–$\theta_{\max}$, for a beam energy E, was calculated as

$$\theta_{\max} = \sin^{-1}\sqrt{\left(\frac{\delta E}{E}\right)} \tag{2}$$

and the results are shown in table 1. Note also that in our experimental technique, positrons scattered in the backward direction, i.e. at angles ($90^\circ < \theta < 180^\circ$), exit the gas cell, are reflected from the potential wall due to the last electrode of the buffer-gas trap, and can pass through the gas cell once more.

Therefore, the missing part of the distribution will extend from 0° to $\theta_{\max}$ and $(180 - \theta_{\max})^\circ$ to 180°. However, as both equation (2) and table 1 show, our angular resolution becomes better

with increasing impact energy. The amount by which both the present GTCS and GTCS $- Q_{Ps}$ results are underestimated due to these missing angles will not be accurately known until there are reliable experimental elastic DCS for each of these two molecules. Schwinger multichannel calculations for positron scattering from HCOOH [31] and R-matrix calculations for positron scattering from H_2O [32] have been made available to us. According to these results for HCOOH, as expected for these highly polar molecules, the positron DCS are as highly forward-peaked as their electron counterparts [33] for energies up to 10 eV, suggesting that we are underestimating the GTCS by about 45% at 4 eV, for example. A similar picture was obtained for H_2O, where the elastic DCS suggested that we are underestimating the GTCS by about 67% at 0.5 eV and 53% at 5 eV. That is, the systematic error involved in our GTCS results at these lower energies is expected to be significant. However, as the impact energy increases above about 10 eV, this systematic error due to the missing angles is expected to become negligible according to equation (2), albeit depending on the behavior of the DCS. It is important to note, however, that these forward scattering problems only affect the elastic scattering component of the cross sections. As such, only the GTCS and GTCS $- Q_{Ps}$ are affected but not the Q_{Ps}. Full results of this forward scattering effect analysis will be discussed in section 4.

The error estimates for the data presented in tables 2–7 and figures 1–8 for the present measurements are the total uncertainties, which are almost entirely due to statistical fluctuations in the measured positron current signals. These errors amount to $<1.6\%$ for GTCS and GTCS $- Q_{Ps}$, and $<8\%$ for Q_{Ps} data of HCOOH, and amount to $<6\%$ for all of these three data sets in H_2O. The magnetic fields in the trap, scattering region and at the retarding potential analyzer are all 530 Gauss and, consequently, corrections due to the helical path length through the cell are small ($\sim 1\%$ at 1 eV scattering energy and reducing as the energy increases), and have not been applied to the data. The other sources of error in the determination of the cross-section magnitude lie in the determination of the number density and path length, and are estimated to be $<1\%$ in this case.

3. Results and discussion

The numerical results for the cross sections for positron scattering are shown in tables 2–4 for H_2O and tables 5–7 for HCOOH, respectively. The order of the discussion that follows is that the GTCS, GTCS $- Q_{Ps}$ and Q_{Ps} results are presented for each molecule separately, in comparison with data from the literature. This is followed by discussions of the behavior of the cross sections at and near the thresholds for ionization and Ps formation. A comparative study of the Q_{Ps} for these two molecules is then carried out, before finishing off with a discussion of the results after the forward scattering effect correction has been made.

3.1. H_2O cross sections

3.1.1. GTCS and GTCS $- Q_{Ps}$. Figure 1 shows a plot of the present GTCS and GTCS $- Q_{Ps}$ results for positron scattering from H_2O, with earlier experimental results due to Kimura *et al* [13], Zecca *et al* [14], Beale *et al* [15], and the theoretical elastic integral cross sections (ECS) of Gianturco *et al* [34] and Baluja *et al* [19, 35].

It is worth noting here that the results of Kimura *et al* presented in figure 1 are the results of Sueoka *et al* [11, 12], after a forward scattering correction using electron impact elastic differential cross sections (DCS). This approach was adopted at that time simply

Table 2. H_2O positron impact GTCS (10^{-16} cm^2). Numbers in parentheses are the values after the forward scattering effect correction. Errors are as explained in the text.

Energy (eV)	GTCS	Energy (eV)	GTCS
0.5	63.756(194.45) ± 1.148(3.50)	25	8.985(11.38) ± 0.119(0.15)
0.75	50.348(151.73) ± 1.019(3.07)	26	8.598(10.81) ± 0.120(0.15)
1	39.751(128.87) ± 1.050(3.40)	27	8.694(10.86) ± 0.125(0.16)
1.25	35.157(115.00) ± 1.080(3.53)	28	8.569(10.64) ± 0.136(0.17)
1.5	29.762(95.30) ± 1.076(3.45)	29	8.432(10.41) ± 0.125(0.15)
1.75	28.941(89.61) ± 1.057(3.27)	30	8.361(10.26) ± 0.060(0.07)
2	22.882(68.20) ± 0.473(1.41)	31	8.307(10.14) ± 0.058(0.07)
2.25	23.941(68.63) ± 1.043(2.99)	32	8.394(10.20) ± 0.061(0.07)
2.5	19.648(54.22) ± 0.469(1.30)	33	8.279(10.01) ± 0.059(0.07)
3	16.658(42.82) ± 0.516(1.33)	34	8.160(9.82) ± 0.072(0.09)
3.5	14.744(35.57) ± 0.511(1.23)	35	8.121(9.73) ± 0.071(0.09)
4	14.539(33.17) ± 0.493(1.13)	36	8.136(9.71) ± 0.068(0.08)
4.5	12.886(27.99) ± 0.499(1.08)	37	8.091(9.62) ± 0.067(0.08)
5	11.141(23.16) ± 0.130(0.27)	38	8.086(9.58) ± 0.068(0.08)
5.5	11.466(22.93) ± 0.503(1.01)	39	7.921(9.35) ± 0.068(0.08)
6	10.951(21.14) ± 0.130(0.25)	40	7.916(9.32) ± 0.068(0.08)
6.5	10.850(20.30) ± 0.470(0.88)	41	7.897(9.27) ± 0.067(0.08)
7	10.462(19.03) ± 0.125(0.23)	42	7.892(9.23) ± 0.067(0.08)
7.5	10.325(18.30) ± 0.478(0.85)	43	7.910(9.23) ± 0.066(0.08)
8	10.066(17.42) ± 0.136(0.24)	44	7.879(9.16) ± 0.068(0.08)
9	9.879(16.40) ± 0.130(0.22)	45	7.766(9.01) ± 0.066(0.08)
10	9.813(15.72) ± 0.127(0.20)	46	7.706(8.92) ± 0.067(0.08)
11	9.446(14.68) ± 0.135(0.21)	47	7.776(8.98) ± 0.065(0.08)
12	9.509(14.38) ± 0.133(0.20)	48	7.574(8.72) ± 0.064(0.07)
13	9.203(13.60) ± 0.129(0.19)	49	7.672(8.82) ± 0.065(0.07)
14	9.305(13.47) ± 0.133(0.19)	50	7.507(8.61) ± 0.066(0.08)
15	9.191(13.06) ± 0.132(0.19)	51	7.574(8.67) ± 0.067(0.08)
16	9.103(12.72) ± 0.139(0.19)	52	7.533(8.60) ± 0.069(0.08)
17	9.172(12.62) ± 0.135(0.19)	53	7.499(8.55) ± 0.068(0.08)
18	8.991(12.20) ± 0.130(0.18)	54	7.490(8.52) ± 0.065(0.07)
19	9.009(12.08) ± 0.130(0.17)	55	7.490(8.50) ± 0.067(0.08)
20	8.967(11.88) ± 0.133(0.18)	56	7.373(8.36) ± 0.063(0.07)
21	8.849(11.61) ± 0.134(0.18)	57	7.382(8.35) ± 0.062(0.07)
22	8.666(11.26) ± 0.123(0.16)	58	7.339(8.29) ± 0.060(0.07)
23	8.825(11.36) ± 0.129(0.17)	59	7.380(8.32) ± 0.056(0.06)
24	8.659(11.05) ± 0.120(0.15)	60	7.292(8.21) ± 0.061(0.07)

because positron elastic DCS were unavailable. As such, the Kimura *et al* data represent that group's preferred results for this target. Therefore, in the discussions that follow we only make comparison with their data. The present GTCS data monotonically decrease from 0.5 eV (∼63.76 Å^2) until our highest energy of 60 eV (∼7.29 Å^2). Similarly, the GTCS − Q_{Ps} data show a smooth energy dependence trend. It is characterized by the decreasing trend from

Table 3. H_2O positron impact GTCS $- Q_{Ps}$ (10^{-16} cm^2). Numbers in parentheses are the values after the forward scattering effect correction. Errors are as explained in the text.

Energy (eV)	GTCS $- Q_{Ps}$	Energy (eV)	GTCS $- Q_{Ps}$
5	11.194(23.27) ± 0.088(0.18)	33	6.172(7.46) ± 0.040(0.05)
6	10.244(19.78) ± 0.087(0.17)	34	6.129(7.38) ± 0.045(0.05)
7	9.044(16.45) ± 0.082(0.15)	35	6.153(7.37) ± 0.046(0.05)
8	8.390(14.52) ± 0.085(0.15)	36	6.178(7.38) ± 0.045(0.05)
9	7.721(12.82) ± 0.085(0.14)	37	6.158(7.32) ± 0.045(0.05)
10	7.408(11.87) ± 0.087(0.14)	38	6.238(7.39) ± 0.044(0.05)
11	7.032(10.92) ± 0.089(0.14)	39	6.154(7.27) ± 0.044(0.05)
12	6.864(10.38) ± 0.088(0.13)	40	6.215(7.31) ± 0.044(0.05)
13	6.527(9.64) ± 0.084(0.12)	41	6.197(7.27) ± 0.046(0.05)
14	6.556(9.49) ± 0.089(0.13)	42	6.193(7.24) ± 0.045(0.05)
15	6.293(8.94) ± 0.086(0.12)	43	6.274(7.32) ± 0.043(0.05)
16	6.308(8.81) ± 0.086(0.12)	44	6.233(7.25) ± 0.045(0.05)
17	6.380(8.78) ± 0.086(0.12)	45	6.235(7.23) ± 0.043(0.05)
18	6.272(8.51) ± 0.085(0.12)	46	6.225(7.20) ± 0.045(0.05)
19	6.233(8.36) ± 0.084(0.11)	47	6.258(7.22) ± 0.045(0.05)
20	6.269(8.31) ± 0.090(0.12)	48	6.184(7.12) ± 0.044(0.05)
21	6.183(8.11) ± 0.083(0.11)	49	6.263(7.20) ± 0.044(0.05)
22	6.023(7.82) ± 0.083(0.11)	50	6.209(7.12) ± 0.045(0.05)
23	6.201(7.98) ± 0.085(0.11)	51	6.316(7.23) ± 0.044(0.05)
24	6.072(7.75) ± 0.084(0.11)	52	6.245(7.13) ± 0.046(0.05)
25	6.346(8.04) ± 0.082(0.10)	53	6.262(7.14) ± 0.046(0.05)
26	6.119(7.70) ± 0.083(0.10)	54	6.262(7.12) ± 0.042(0.05)
27	6.304(7.87) ± 0.083(0.10)	55	6.272(7.12) ± 0.046(0.05)
28	6.091(7.56) ± 0.088(0.11)	56	6.240(7.07) ± 0.044(0.05)
29	6.202(7.65) ± 0.087(0.11)	57	6.201(7.02) ± 0.044(0.05)
30	6.094(7.48) ± 0.040(0.05)	58	6.225(7.03) ± 0.042(0.05)
31	6.088(7.43) ± 0.038(0.05)	59	6.264(7.06) ± 0.042(0.05)
32	6.202(7.53) ± 0.040(0.05)	60	6.215(7.00) ± 0.046(0.05)

5.0 eV until it almost flattens off above 15 eV. That the present GTCS results, and those of Zecca *et al*, rise significantly in magnitude as the positron energy is decreased toward 0 eV points to the importance of long-range polarization effects and/or water's permanent dipole moment at these lower energies. The current GTCS values are in good agreement with those of Zecca *et al* [14] up to ∼8 eV. Above this energy the current results are larger in magnitude than the Zecca *et al* result, with the difference increasing with increasing impact energy, to a maximum of ∼12% at their maximum energy point. It is likely that this difference simply reflects small differences in their respective energy-dependent angular resolutions. With our experimental technique the angular resolution becomes better with increasing energy, as can be seen in equation (2). The present measured GTCS data differ from those of Beale *et al* [15] by about a factor of two over all the energy range of overlap, probably also because of angular resolution. Below 5 eV, the present results are lower than both the

Table 4. H_2O positron impact Q_{Ps} (10^{-16} cm^2). Errors are as explained in the text.

Energy (eV)	Q_{Ps}	Energy (eV)	Q_{Ps}
5	-0.001 ± 0.101	33	2.108 ± 0.044
6	0.750 ± 0.103	34	2.040 ± 0.055
7	1.448 ± 0.104	35	1.974 ± 0.055
8	1.683 ± 0.103	36	1.965 ± 0.053
9	2.174 ± 0.104	37	1.942 ± 0.053
10	2.418 ± 0.106	38	1.853 ± 0.052
11	2.425 ± 0.101	39	1.772 ± 0.053
12	2.665 ± 0.103	40	1.708 ± 0.053
13	2.686 ± 0.104	41	1.704 ± 0.053
14	2.756 ± 0.102	42	1.707 ± 0.053
15	2.918 ± 0.104	43	1.644 ± 0.051
16	2.813 ± 0.104	44	1.657 ± 0.051
17	2.820 ± 0.109	45	1.538 ± 0.050
18	2.736 ± 0.102	46	1.492 ± 0.052
19	2.804 ± 0.107	47	1.527 ± 0.049
20	2.726 ± 0.105	48	1.397 ± 0.050
21	2.696 ± 0.105	49	1.417 ± 0.050
22	2.664 ± 0.102	50	1.305 ± 0.050
23	2.650 ± 0.103	51	1.267 ± 0.052
24	2.593 ± 0.092	52	1.300 ± 0.051
25	2.672 ± 0.098	53	1.248 ± 0.050
26	2.495 ± 0.096	54	1.238 ± 0.049
27	2.424 ± 0.099	55	1.228 ± 0.048
28	2.519 ± 0.100	56	1.141 ± 0.048
29	2.253 ± 0.099	57	1.192 ± 0.046
30	2.278 ± 0.048	58	1.124 ± 0.045
31	2.229 ± 0.047	59	1.124 ± 0.044
32	2.206 ± 0.047	60	1.088 ± 0.041

close-coupling ECS results calculated by Gianturco *et al* [34], using a parameter-free quantum dynamical model for the electron–positron correlations, and those by Baluja *et al* [19], who performed their calculations within the fixed-nuclei approximation, corrected with the standard Born-closure formula. The present results also differ qualitatively and quantitatively from the theoretical ECS calculations of Baluja and Jain [35] who used a spherical-complex-optical-potential method. In addition, although it is not included in the plot for reasons of clarity, there is another calculation by De-Heng *et al* [36], which agrees very well with the Beale *et al* [15] data, but also differs from the present results. These authors employed a complex-optical-potential approach and applied the additivity rule to sum the cross sections calculated for the constituent atoms. It is intriguing to note that above 10 eV the present GTCS $- Q_{Ps}$ data agree in both magnitude and energy dependence with the GTCS data of Beale *et al* [15]. This could be fortuitous, given that these two results are not corrected for the forward scattering effect. The result of Kimura *et al* is greater than the present GTCS results over all the energy

Table 5. HCOOH positron impact GTCS (10^{-16} cm^2). Numbers in parentheses are the values after the forward scattering effect correction. Errors are as explained in the text.

Energy (eV)	GTCS	Energy (eV)	GTCS
4	17.754(31.54) ± 0.175(0.31)	25	15.378(15.51) ± 0.145(0.15)
4.2	17.766(30.95) ± 0.193(0.32)	26	15.480(15.57) ± 0.234(0.24)
4.4	17.617(30.08) ± 0.197(0.31)	27	15.151(15.26) ± 0.225(0.24)
4.6	17.331(29.02) ± 0.195(0.29)	28	15.405(15.50) ± 0.245(0.24)
4.8	17.451(28.62) ± 0.188(0.26)	29	15.240(15.39) ± 0.240(0.24)
5	17.522(28.13) ± 0.189(0.25)	30	15.463(15.59) ± 0.232(0.24)
5.2	17.499(27.57) ± 0.205(0.25)	31	15.100(15.25) ± 0.234(0.24)
5.4	17.523(27.05) ± 0.194(0.25)	32	15.292(15.43) ± 0.229(0.23)
5.6	17.851(27.01) ± 0.197(0.24)	33	15.438(15.58) ± 0.229(0.23)
5.8	17.506(25.94) ± 0.188(0.23)	34	15.316(15.45) ± 0.225(0.23)
6	17.634(25.58) ± 0.195(0.23)	35	14.715(14.84) ± 0.223(0.23)
6.2	17.609(25.12) ± 0.187(0.23)	36	15.167(15.32) ± 0.219(0.23)
6.4	17.639(24.75) ± 0.195(0.23)	37	15.178(15.33) ± 0.224(0.24)
6.6	17.453(24.08) ± 0.185(0.22)	38	14.890(15.04) ± 0.224(0.23)
6.8	17.551(23.80) ± 0.187(0.22)	39	14.655(14.81) ± 0.229(0.24)
7	17.238(22.94) ± 0.143(0.17)	40	14.827(14.97) ± 0.228(0.23)
7.2	17.333(22.90) ± 0.171(0.20)	41	14.933(15.14) ± 0.222(0.23)
7.4	17.670(23.16) ± 0.162(0.20)	42	14.549(14.70) ± 0.231(0.24)
7.6	17.391(22.61) ± 0.158(0.19)	43	14.589(14.75) ± 0.215(0.22)
7.8	17.223(22.20) ± 0.148(0.18)	44	14.489(14.68) ± 0.225(0.23)
8	17.252(22.01) ± 0.125(0.15)	45	14.234(14.37) ± 0.214(0.22)
9	16.575(20.23) ± 0.231(0.28)	46	14.394(14.59) ± 0.226(0.23)
10	16.347(19.03) ± 0.260(0.28)	47	14.246(14.43) ± 0.202(0.21)
11	16.601(18.84) ± 0.252(0.26)	48	13.867(14.00) ± 0.217(0.22)
12	16.216(17.92) ± 0.178(0.19)	49	14.058(14.22) ± 0.211(0.21)
13	16.480(17.64) ± 0.176(0.19)	50	13.784(13.96) ± 0.217(0.23)
14	16.327(17.00) ± 0.161(0.17)	51	14.014 ± 0.207
15	16.366(16.52) ± 0.160(0.16)	52	13.886 ± 0.216
16	15.551(15.74) ± 0.253(0.27)	53	13.607 ± 0.211
17	15.762(15.92) ± 0.258(0.25)	54	13.613 ± 0.211
18	15.550(15.67) ± 0.229(0.24)	55	13.449 ± 0.215
19	15.349(15.45) ± 0.262(0.27)	56	13.579 ± 0.211
20	15.488(15.60) ± 0.240(0.25)	57	13.608 ± 0.199
21	15.480(15.59) ± 0.203(0.22)	58	13.282 ± 0.199
22	15.343(15.46) ± 0.218(0.23)	59	13.504 ± 0.193
23	15.354(15.45) ± 0.234(0.23)	60	13.375 ± 0.172
24	15.379(15.44) ± 0.152(0.16)		

Table 6. HCOOH positron impact GTCS $- Q_{Ps}$ (10^{-16} cm^2). Numbers in parentheses are the values after the forward scattering effect correction. Errors are as explained in the text.

Energy (eV)	GTCS $- Q_{Ps}$	Energy (eV)	GTCS $- Q_{Ps}$
4	18.009(31.99) ± 0.112(0.20)	25	10.868(10.97) ± 0.100(0.10)
4.2	17.786(31.13) ± 0.105(0.18)	26	11.006(11.11) ± 0.130(0.13)
4.4	17.620(30.38) ± 0.114(0.20)	27	10.934(11.04) ± 0.137(0.14)
4.6	17.025(28.90) ± 0.109(0.18)	28	11.084(11.20) ± 0.132(0.13)
4.8	16.706(27.93) ± 0.110(0.18)	29	10.980(11.09) ± 0.137(0.14)
5	16.426(27.03) ± 0.115(0.19)	30	11.262(11.38) ± 0.133(0.13)
5.2	16.018(25.99) ± 0.117(0.19)	31	11.065(11.18) ± 0.141(0.14)
5.4	15.667(25.06) ± 0.106(0.17)	32	11.114(11.24) ± 0.134(0.14)
5.6	15.633(24.65) ± 0.112(0.18)	33	11.333(11.46) ± 0.138(0.14)
5.8	15.054(23.39) ± 0.109(0.17)	34	11.341(11.47) ± 0.126(0.13)
6	14.960(22.90) ± 0.114(0.18)	35	11.068(11.19) ± 0.130(0.13)
6.2	14.637(22.08) ± 0.121(0.18)	36	11.442(11.58) ± 0.136(0.14)
6.4	14.426(21.45) ± 0.119(0.18)	37	11.357(11.49) ± 0.129(0.13)
6.6	14.101(20.65) ± 0.115(0.17)	38	11.468(11.61) ± 0.123(0.12)
6.8	14.030(20.24) ± 0.115(0.17)	39	11.251(11.39) ± 0.139(0.14)
7	13.595(19.31) ± 0.085(0.12)	40	11.466(11.61) ± 0.129(0.13)
7.2	13.590(19.16) ± 0.118(0.17)	41	11.573(11.72) ± 0.131(0.13)
7.4	13.666(19.12) ± 0.111(0.16)	42	11.466(11.61) ± 0.142(0.14)
7.6	13.355(18.54) ± 0.113(0.16)	43	11.395(11.54) ± 0.126(0.13)
7.8	13.219(18.21) ± 0.110(0.15)	44	11.541(11.69) ± 0.135(0.14)
8	13.068(17.86) ± 0.086(0.12)	45	11.368(11.51) ± 0.128(0.13)
9	12.198(15.83) ± 0.136(0.18)	46	11.548(11.70) ± 0.138(0.14)
10	11.765(14.45) ± 0.158(0.19)	47	11.549(11.70) ± 0.121(0.12)
11	11.695(13.88) ± 0.158(0.19)	48	11.149(11.29) ± 0.133(0.13)
12	11.454(13.12) ± 0.100(0.11)	49	11.446(11.60) ± 0.131(0.13)
13	11.282(12.45) ± 0.117(0.13)	50	11.301(11.45) ± 0.135(0.14)
14	11.128(11.82) ± 0.106(0.11)	51	11.650 ± 0.126
15	11.234(11.47) ± 0.109(0.11)	52	11.570 ± 0.133
16	10.749(10.95) ± 0.150(0.15)	53	11.369 ± 0.126
17	10.919(11.10) ± 0.147(0.15)	54	11.464 ± 0.134
18	10.892(11.04) ± 0.148(0.15)	55	11.391 ± 0.130
19	10.519(10.63) ± 0.166(0.17)	56	11.601 ± 0.130
20	10.817(10.91) ± 0.153(0.15)	57	11.596 ± 0.129
21	10.805(10.90) ± 0.128(0.13)	58	11.427 ± 0.140
22	10.769(10.86) ± 0.138(0.14)	59	11.445 ± 0.133
23	10.771(10.87) ± 0.147(0.15)	60	11.505 ± 0.132
24	10.726(10.83) ± 0.097(0.10)		

Table 7. HCOOH positron impact Q_{Ps} (10^{-16} cm^2). Errors are as explained in the text.

Energy (eV)	Q_{Ps}	Energy (eV)	Q_{Ps}
4	-0.240 ± 0.166	25	4.533 ± 0.106
4.2	-0.008 ± 0.160	26	4.456 ± 0.198
4.4	0.012 ± 0.166	27	4.216 ± 0.195
4.6	0.315 ± 0.162	28	4.301 ± 0.199
4.8	0.755 ± 0.158	29	4.292 ± 0.197
5	1.103 ± 0.157	30	4.213 ± 0.193
5.2	1.499 ± 0.166	31	4.064 ± 0.190
5.4	1.865 ± 0.166	32	4.192 ± 0.192
5.6	2.230 ± 0.163	33	4.124 ± 0.187
5.8	2.462 ± 0.154	34	3.982 ± 0.193
6	2.681 ± 0.153	35	3.647 ± 0.191
6.2	2.977 ± 0.149	36	3.748 ± 0.184
6.4	3.220 ± 0.153	37	3.840 ± 0.197
6.6	3.356 ± 0.150	38	3.435 ± 0.189
6.8	3.531 ± 0.149	39	3.419 ± 0.192
7	3.633 ± 0.121	40	3.362 ± 0.186
7.2	3.748 ± 0.124	41	3.421 ± 0.193
7.4	4.009 ± 0.130	42	3.089 ± 0.187
7.6	4.040 ± 0.118	43	3.204 ± 0.183
7.8	4.002 ± 0.108	44	2.992 ± 0.186
8	4.150 ± 0.094	45	2.860 ± 0.175
9	4.369 ± 0.201	46	2.898 ± 0.187
10	4.577 ± 0.196	47	2.729 ± 0.169
11	4.911 ± 0.177	48	2.709 ± 0.173
12	4.771 ± 0.146	49	2.628 ± 0.167
13	5.138 ± 0.143	50	2.507 ± 0.189
14	5.149 ± 0.127	51	2.383 ± 0.176
15	5.047 ± 0.109	52	2.321 ± 0.173
16	4.790 ± 0.224	53	2.231 ± 0.168
17	4.824 ± 0.196	54	2.166 ± 0.168
18	4.636 ± 0.192	55	2.032 ± 0.170
19	4.811 ± 0.212	56	2.015 ± 0.162
20	4.694 ± 0.193	57	2.030 ± 0.158
21	4.692 ± 0.175	58	1.887 ± 0.150
22	4.596 ± 0.186	59	2.109 ± 0.145
23	4.579 ± 0.178	60	1.889 ± 0.119
24	4.611 ± 0.121		

range of overlap. However, it is not appropriate to discuss the comparison between these two results here because, as highlighted above, the Kimura *et al* data have been corrected for forward scattering effects whereas the present data are not. We therefore defer discussion of the comparison with their data to section 4, where their data will be compared with our data after correction for the forward scattering effect.

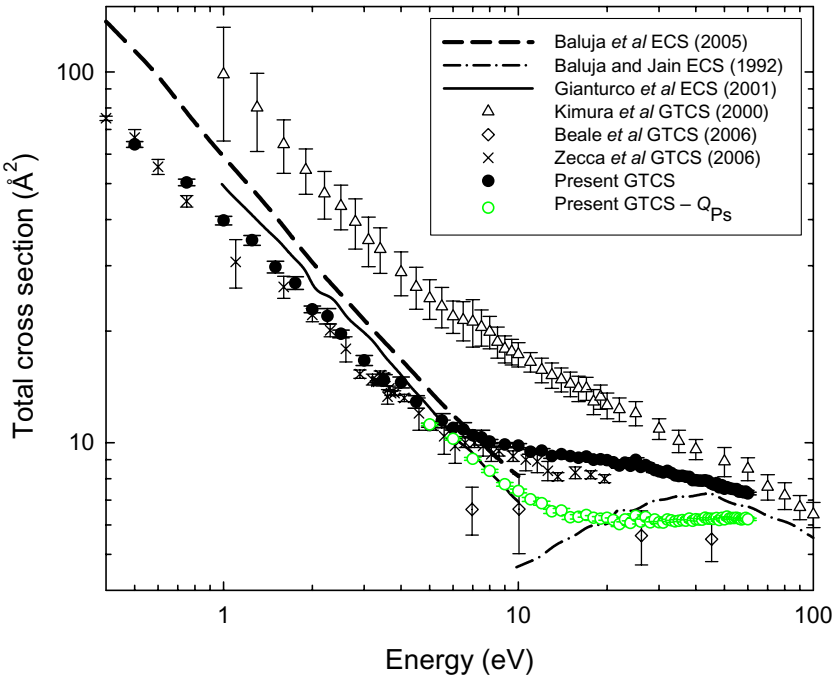

Figure 1. Present positron impact H_2O GTCS and GTCS $- Q_{Ps}$ compared with the literature for GTCS and elastic integral cross section (ECS) results.

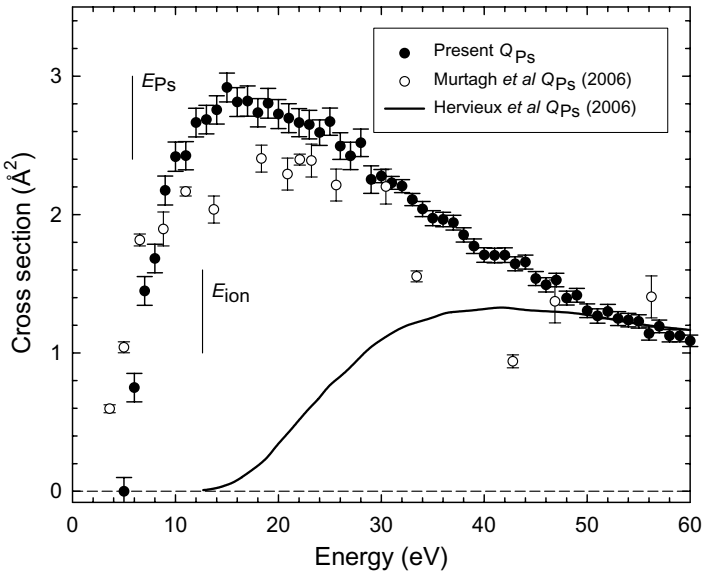

Figure 2. Present positron impact H_2O Q_{Ps} results compared with literature experimental and theoretical results.

3.1.2. Positronium formation cross sections: Q_{Ps}. Figure 2 shows the present Q_{Ps} data in comparison with the preliminary experimental results of Murtagh *et al* [16] and the theoretical results of Hervieux *et al* [18]. The latter authors employed the so-called independent electron model in which the wavefunction of the water molecule was described by a linear combination

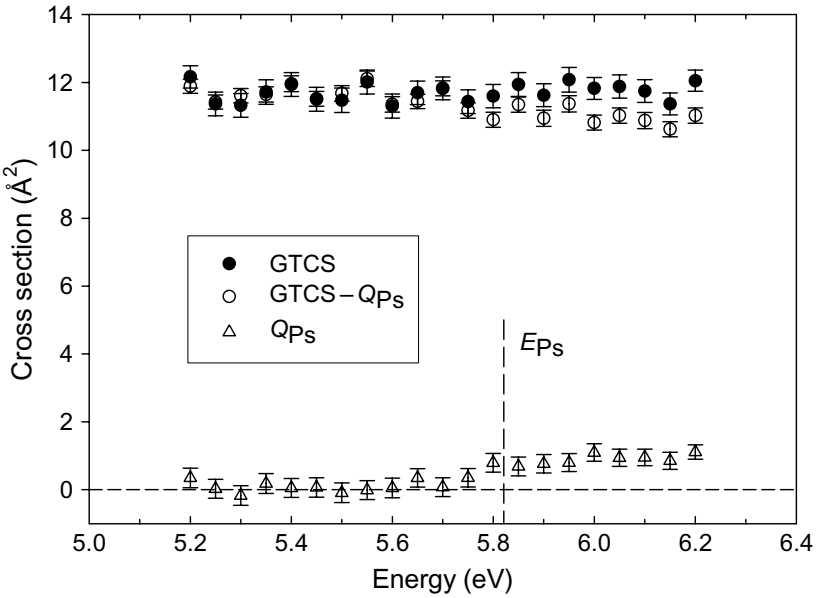

Figure 3. Present positron impact H_2O GTCS, GTCS $- Q_{Ps}$ and Q_{Ps} results in the vicinity of the Ps threshold ($E_{Ps} = 5.821$ eV).

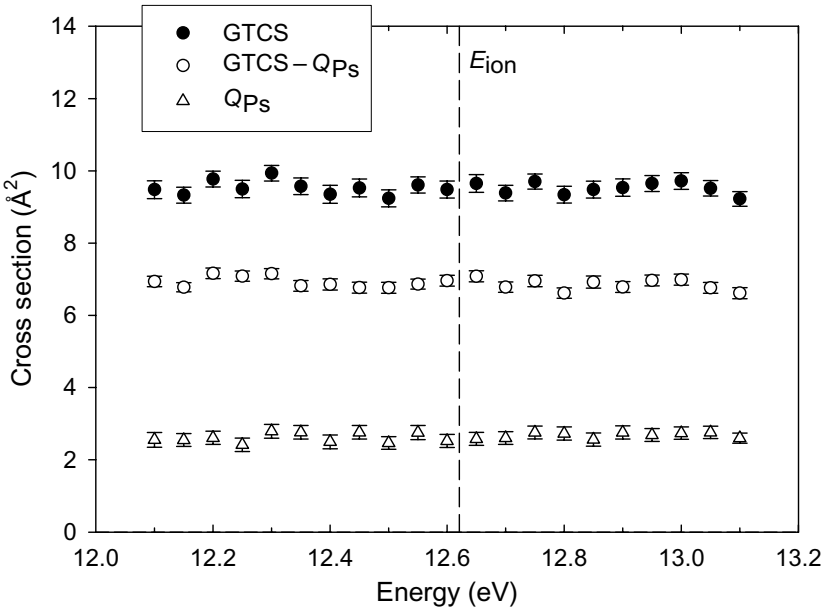

Figure 4. Same as figure 3 but in the vicinity of the ionization threshold ($E_{ion} = 12.621$ eV).

of atomic orbitals centered on the oxygen atom. In their Q_{Ps} determination, Hervieux *et al* [18] evaluate contributions from different initial molecular orbitals. They present Q_{Ps} data for ground state Ps formation (Ps(1s)), and Ps formation in the 2s excited states (Ps(2s)). Their data shown in figure 2 represent their total Q_{Ps}, i.e. for Ps(1s) + Ps(2s). Our measured Q_{Ps} data, and those of Murtagh *et al* [16], represent the sum of all possible Ps formation pathways.

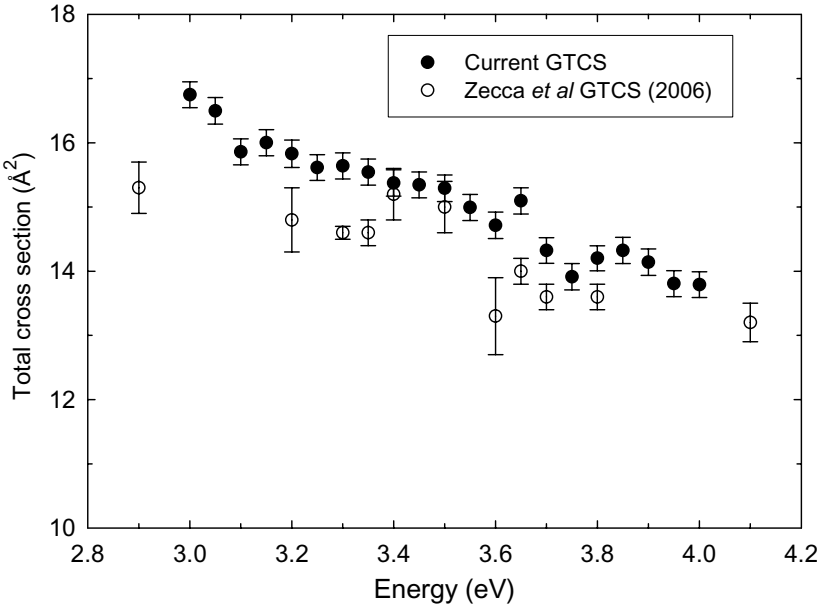

Figure 5. Present positron impact H_2O GTCS results compared with those of Zecca *et al* below E_{Ps}.

There is a fair agreement between the present results and those of the UCL group, Murtagh *et al*, for the energy dependence of Q_{Ps} below 45 eV, albeit with some subtle qualitative and quantitative differences. The threshold for Ps formation in H_2O, E_{Ps}, is at 5.821 eV. The results by the UCL group show a nonzero Q_{Ps} value at their lowest energy of 4 eV. In contrast, the current results show a cross section of $\sim$0 Å^2 at 5 eV, i.e. the lowest energy point presented in this figure. Both results show the broad peak in the cross-section spanning the energy range of $\sim$10–30 eV, albeit with varying magnitude differences, amounting to $\sim$30% at 14 eV, and increasing to $\sim$70% at 43 eV. The difference between the current results and the theoretical values of Hervieux *et al* is obvious below 50 eV. Above this energy, however, there is better agreement as the theoretical result crosses over the current Q_{Ps} curve to become larger in magnitude. An intriguing observation is that these theoretical Q_{Ps} data show an E_{Ps} of $\sim$12.7 eV. That the theoretical E_{Ps} is almost equal to the ionization potential of the highest occupied molecular orbital in H_2O ($E_{ion} = 12.621$ eV) perhaps highlights one of the common problems that theory has in handling Ps formation below E_{ion}. In this region the Ps formation channel competes with the elastic and any open inelastic channel, making it difficult for theoretical treatments as this requires a two-centre expansion for accurate calculations. However, even above the E_{ion}, the theoretical values are considerably smaller than the current Q_{Ps} values below 50 eV.

3.1.3. Ps formation and ionization threshold regions. In figures 3 and 4, we present GTCS, GTCS $- Q_{Ps}$ and Q_{Ps} results in the vicinity of E_{Ps} and E_{ion} for H_2O. In particular, the energy region from E_{Ps} through to the first electronic excitation energy, called the Ore-gap, is of interest to us following predictions and/or observations of channel coupling effects in similar regions in He [37] and Ar and Xe [38].

In principle, there is a chance of these effects occurring at the opening of every inelastic channel, and thus our choice of the current measurements around E_{Ps} and E_{ion}, which are

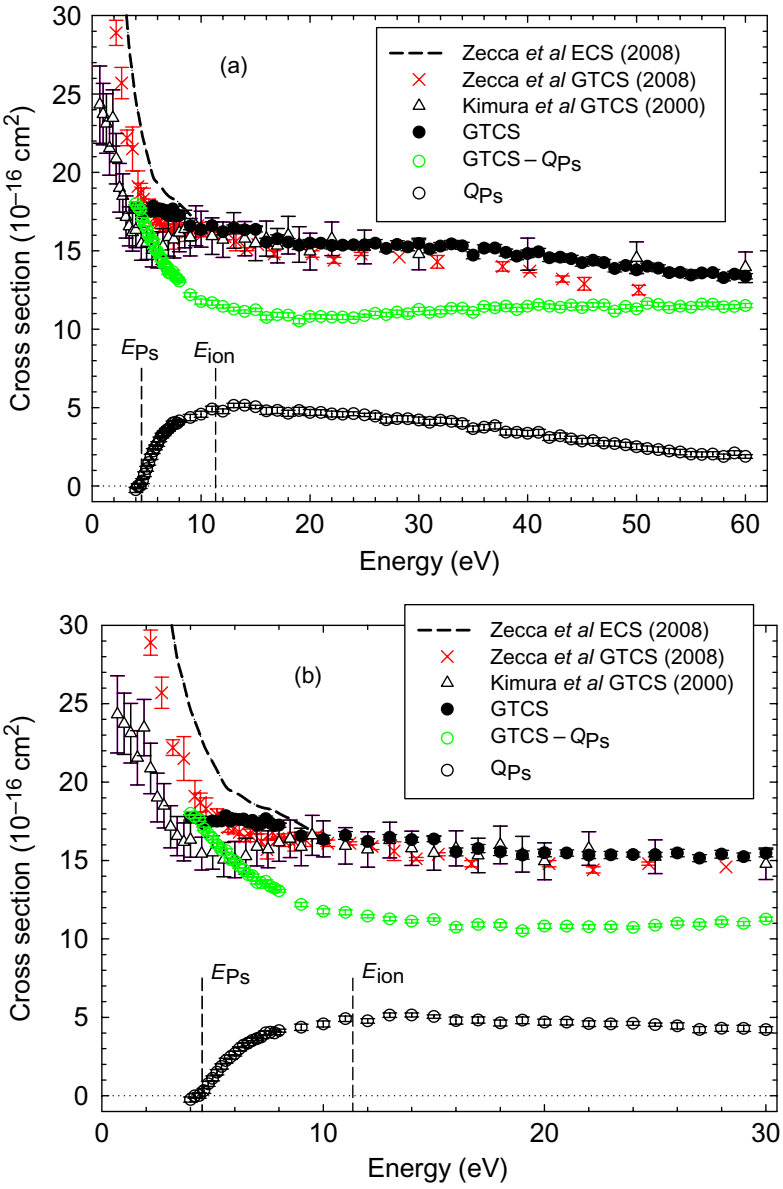

Figure 6. Present positron impact HCOOH GTCS, GTCS $- Q_{Ps}$ and Q_{Ps} compared with literature for GTCS and elastic integral (ECS) results (a) over the whole energy range of measurement and (b) below 30 eV.

expected to be the most significant in terms of the size of the cross-section contribution to the GTCS. Conclusions on the existence of these effects have been drawn from the observed ∼25% decrease in GTCS $- Q_{Ps}$ data in the Ore-gap to produce the reported cusp in He [37], and the sharp (∼50%) rise in GTCS $- Q_{Ps}$ in the Ore-gap observed in Ar and Xe [38], where it was attributed to virtual Ps formation. Figure 3 shows that the Ps formation channel opens up and increases smoothly in cross-section magnitude with no obvious features. In addition, the GTCS $- Q_{Ps}$ values gradually become smaller than the GTCS values. There is no sudden change of slope in this cross-section curve that would be indicative of any channel coupling effects similar to those reported for He [37] and Ar and Xe [38]. The results in figure 4 again

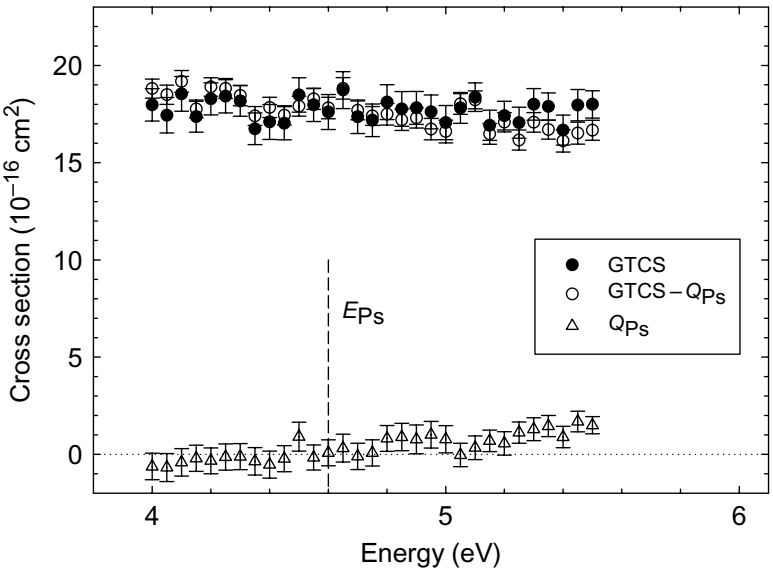

Figure 7. Present positron impact HCOOH GTCS, GTCS $-$ Q_{Ps} and Q_{Ps} results in the vicinity of the Ps threshold ($E_{Ps} = 4.53$ eV).

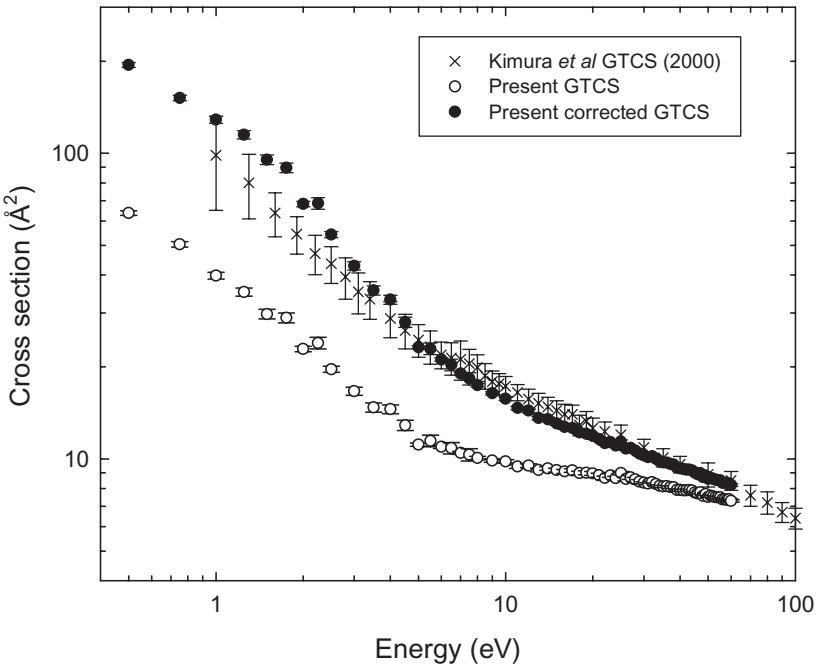

Figure 8. Present positron impact H_2O GTCS before and after correction for the forward scattering effects. Also shown is the GTCS result of Kimura *et al* [13].

show no such signatures of channel coupling around E_{ion}, with all three cross-section curves being almost flat across the whole energy region investigated, i.e. from 0.5 eV below to 0.5 eV above E_{ion}. In addition, based on these GTCS and GTCS $-$ Q_{Ps} data, there is no peak feature in the cross sections that could be interpreted as evidence for any resonances.

3.1.4. The energy region 3–4 eV. In figure 5, we present the current GTCS results, measured with a finer energy increment of 50 meV, over the energy region from 3 to 4 eV, in comparison with similar results by Zecca *et al* [14].

The reason for this investigation is that Zecca *et al* reported a feature centered at ∼3.5 eV, observed as a 10% increase in their GTCS, which they reported to be above their statistical uncertainty, reproducible, and not due to any experimental artifact. This would be an important observation of a resonance feature in positron scattering from H_2O. We also carried out several experimental runs at different times and got reproducible results, whose error-weighted average is shown in figure 5. The present GTCS results do not show the structure observed by these authors at 3.5 eV. However, they do show some structures that are above statistics, centered at ∼3.65 eV and 3.85 eV. Though not shown in the plot, we tried shifting the Zecca *et al* data upwards in energy by 150 meV (which is within their stated uncertainty on their energy calibration) and compared it with the current results. That analysis shows the feature they report falling on and resembling the one we observe at ∼3.65 eV. In addition, their data shows a change of slope that is similar to what we observe at ∼3.85 eV. More experiments are needed, perhaps in discrete scattering channels, to study these features in better detail in order to understand their exact nature and origin. For example, in this energy region where only the elastic scattering channel is open, elastic scattering via resonances is in general masked by the direct elastic component. However, resonances can be clearly revealed in vibrational excitation functions.

3.2. HCOOH cross sections

3.2.1. GTCS, $GTCS - Q_{Ps}$ and Q_{Ps}. Figures 6(a) and (b) show the present results for positron scattering from HCOOH, with earlier experimental GTCS results due to Kimura *et al* [13] and Zecca *et al* [6]. Also included in this plot are the Schwinger multichannel theoretical ECS presented in [6]. The current GTCS and these two previous experimental results have not been corrected for forward scattering effects. The present GTCS result agrees well, within experimental error, with that of Kimura *et al* at all energies of overlap above 8.5 eV, with agreement below this energy being marginal. This contrasts with the agreement seen with the results of Zecca *et al* which is good between about 4 eV and 25 eV, particularly when the total, rather than just statistical, errors on the Trento data are considered. Similar to the case of H_2O the current GTCS results are greater in magnitude than those of Zecca *et al* above 25 eV, with the difference increasing with increasing impact energy, to a maximum of ∼10% at their common maximum energy point. We interpret this difference to be due to the same sort of angular resolution issue highlighted above. In principle, this is the same type of situation for the Kimura *et al* results, so that the broad agreement observed here is much harder to understand.

Figure 6(b) shows the results over the energy region below 30 eV. It is also worth noting that, despite differences in magnitude between the current GTCS results and those of Kimura *et al* below 7.5 eV, their data only exhibit the dipole- and/or polarizability-induced enhancement of the GTCS at energies below 4 eV. Contrary to the current GTCS results, in both the Zecca *et al* and Kimura *et al* data, a minimum, or change of slope, is observable at ∼ 4.3 eV, which they attribute to the opening of the Ps formation channel. In our experimental technique, the GTCS, $GTCS - Q_{Ps}$ and Q_{Ps} data are measured simultaneously, but independently. The lack of an observable change of slope at ∼ 4.5 eV in our GTCS is also consistent with the rapidly decreasing $GTCS - Q_{Ps}$ in combination with the rapidly rising Q_{Ps}. The current GTCS

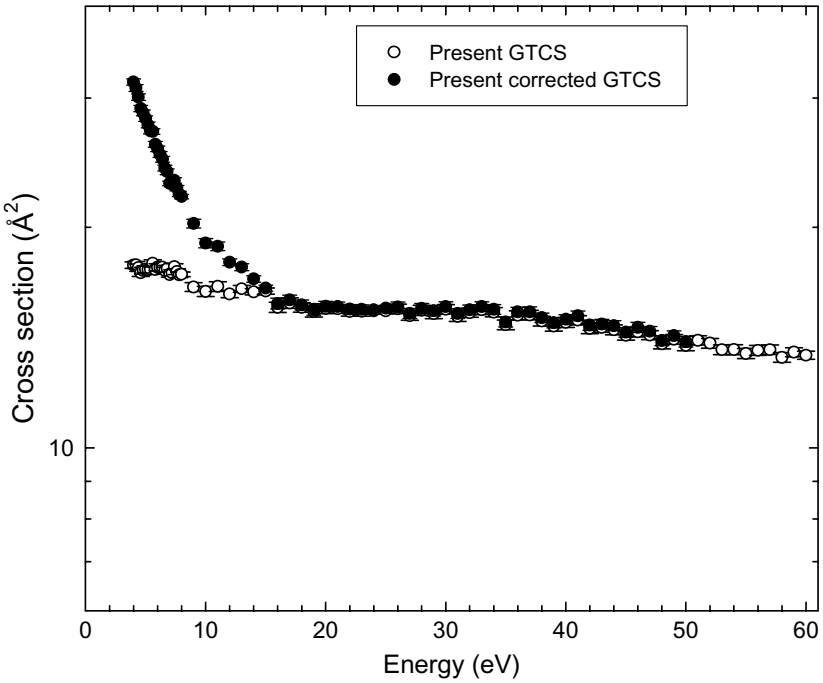

Figure 9. Same caption as figure 8, but now for HCOOH.

results also differ in both magnitude and energy dependence with the Schwinger multichannel theoretical ECS.

The Q_{Ps} data show no peculiar structure across the whole energy range of measurements. It rises rapidly from threshold, at $E_{Ps}(= 4.53\,eV)$ and reaches a maximum at about $E_{ion}(= 11.33\,eV)$. Above 15 eV, it decreases almost linearly all the way to 60 eV. Similarly, the GTCS $- Q_{Ps}$ data is also smooth, decreasing rapidly with increasing energy above E_{Ps}, and then increasing slowly in magnitude above 15 eV. We note that there are no other measurements of calculations that we can compare the present HCOOH Q_{Ps} data against at this time.

3.2.2. Ps formation threshold region. Figure 7 shows the present GTCS, GTCS $- Q_{Ps}$ and Q_{Ps} results in the vicinity of E_{Ps} for HCOOH. We have carried out an investigation similar to that presented for H_2O earlier, searching for any signatures of positron resonances or temporary bound states as this inelastic channel opens up. Over the 4–5.5 eV energy range, the Q_{Ps} results show that the Ps formation channel opens up very slowly. There is no sudden change of slope in the GTCS $- Q_{Ps}$ cross-section curve that would be indicative of any channel coupling or resonance effects.

4. Forward scattering effect correction: GTCS and GTCS $- Q_{Ps}$

Figures 8 and 9 show the results of a forward scattering correction to the GTCS. Note that we have chosen not to plot the GTCS $- Q_{Ps}$ data for reasons of clarity of the graphs, and also since these GTCS $- Q_{Ps}$ cross sections will be changed by the same absolute values as their corresponding GTCS counterparts. As highlighted in section 2, the forward scattering effects are due to positrons elastically scattered into the experimentally inaccessible angular range

$0^\circ - \theta_{max}$, i.e. see equation (2). Therefore this only affects the elastic scattering cross section, by causing it to be underestimated, and thus the correction needs only be done for the measured GTCS and GTCS $- Q_{Ps}$.

The results for both H_2O and HCOOH show that the correction leads to an increase in the GTCS values, with the percentage increase decreasing with increasing impact energy. For H_2O this increase is still 12.5% at 60 eV, i.e. non-negligible. In comparison, the increases in HCOOH are 0.9% at 15 eV, and less than 1% above this energy. That is, the forward scattering correction for HCOOH becomes negligible above 15 eV, but remains significant over all the current energy range for H_2O. As shown in table 1, since the experimental configuration and thus range of missing angles were the same for these two targets, these differences in the correction rates directly reflect on the differences in the magnitude and angular dependence of the elastic DCS for these two targets [31, 32].

In figure 8, we have also included the results of Kimura *et al* [13], i.e. these authors' result after correction for the forward scattering effects in their apparatus. The general qualitative and quantitative agreement between their result and the current corrected GTCS results is very good, but perhaps not surprising. This is because these authors used electron impact H_2O elastic DCS to correct their measured positron GTCS, which we find is quite similar in shape and magnitude to the calculated positron impact elastic DCS that we have employed in the present corrected positron GTCS data.

5. Conclusions

In this paper, we present high energy resolution measurements of GTCS, GTCS $- Q_{Ps}$ and Q_{Ps} results for positron scattering from HCOOH and H_2O molecules over the energy range 4–60 eV and 0.5–60 eV, respectively. The GTCS results for H_2O were characterized by a sharply rising trend below about 6 eV, which was attributed to the dipole moment and/or dipole polarizability for this strongly polar molecule. However, in the limit of the current lowest measurement energy of 4 eV for HCOOH, this effect could not be observed for that molecule. We note that such a strongly increasing GTCS for impact energies below 4 eV was observed by both Kimura *et al* [13] and Zecca *et al* [6] in HCOOH. Measurements have also been carried out to investigate the behavior of GTCS, GTCS $- Q_{Ps}$ and Q_{Ps} in the vicinity of the Ps formation and ionization thresholds. No evidence of channel coupling or resonance features has been observed for either target. The Ps formation cross section has been found to be approximately two times greater in magnitude for HCOOH than H_2O.

Plans are underway to extend these measurements to cover elastic differential cross sections. In addition to the deeper fundamental insight that these can provide, they will also assist in the correct evaluation of the corrections due to forward scattering, that need to be applied to the current GTCS, and GTCS $- Q_{Ps}$, at lower energies. Vibrational excitation cross-section measurements are also planned and these may also prove more conclusive with regard to the existence, or otherwise, of quasi-bound states or resonances.

Another aspect of the work that is under way is the application of the newly measured cross sections in models of positron transport in water vapor and eventually in liquid water. Special properties of such transport phenomena have been found due to large non-conservative Ps formation cross sections in argon and hydrogen [39]–[41]. We may predict, based on the shape of the cross sections only, that the negative differential conductivity (reduction of the drift velocity with the increasing density normalized electric field E/N) will not be as strong as

for argon due to greater relative magnitudes of the grand total and Ps formation cross sections which are less pronounced in H_2O. Whether the effect will exist at all will depend on the relative importance of the inelastic channels such as vibrational excitation, electronic excitations and dissociation to the Ps formation channel. Application of the cross sections found here for the actual liquid medium would require modification of the cross sections mostly at low energies to take into account multiple scattering at high target densities. Thus, one would need an analysis such as that carried out by White and Robson [42] but for polar molecules. Still the high density effects are likely to affect the effective cross sections only at energies lower than the threshold for Ps formation.

Acknowledgments

We acknowledge the funding of the Australian Research Council's Centre of Excellence Program. We are also indebted to Graeme Cornish, Stephen Battisson, Ross Tranter and Ron Cruikshank for their excellent technical skills and on-going support. CM and JPS are grateful to the Australian Research Council for financial support under the APD and ARF programs, respectively. AB and ZP would like to acknowledge funding under the MNTRS 141025 Project. KLN thanks the DIISR for her ISL funding. We thank Dr Marcio H F Bettega and Professor Jonathan Tennyson for carrying out positron elastic DCS calculations, and supplying us with the tabulated data prior to publication, and for useful discussions concerning the results. We are also grateful to Professor Osamu Sueoka for providing us with numerical values of their data presented in this paper.

References

[1] Boudaiffa B, Cloutier P, Hunting D, Huels M A and Sanche L 2000 *Science* **287** 1658
[2] Menichetti L, Cionini L, Sauerwein W A, Altieri S, Solin O, Minn H and Salvadori P A 2009 *Appl. Radiat. Isot.* **67** S351
[3] Bernath P F 2002 *Phys. Chem. Chem. Phys.* **4** 1501
[4] Taylor F W 2002 *Rep. Prog. Phys.* **65** 1
[5] Itikawa Y and Mason N 2005 *J. Phys. Chem. Data* **34** 1
[6] Zecca A, Chiari L, Sarkar A, Lima M A P, Bettega M H F, Nixon K L and Brunger M J 2008 *Phys. Rev.* A **78** 042707
[7] Alvarado F, Hoekstra R and Schlatholter T 2005 *J. Phys. B: At. Mol. Opt. Phys.* **38** 4085
[8] Strauss L G and Conti P S 1991 *J. Nucl. Med.* **32** 623
[9] Aouchiche H, Champion C and Oubaziz D 2008 *Rad. Phys. Chem.* **77** 107
[10] Surko C M, Gribakin G F and Buckman S J 2005 *J. Phys. B: At. Mol. Opt. Phys.* **38** R35
[11] Sueoka O, Mori S and Katayama Y 1986 *J. Phys. B: At. Mol. Phys.* **19** L373
[12] Sueoka O, Mori S and Katayama Y 1987 *J. Phys. B: At. Mol. Phys.* **20** 3237
[13] Kimura M, Sueoka O, Hamada A and Itikawa Y 2000 *Adv. Chem. Phys.* **111** 537
[14] Zecca A, Sanyal D, Chakrabarti M and Brunger M J 2006 *J. Phys. B: At. Mol. Opt. Phys.* **39** 1597
[15] Beale J, Armitage S and Laricchia G 2006 *J. Phys. B: At. Mol. Opt. Phys.* **39** 1337
[16] Murtagh D J, Arcidiacono C, Pesic Z D and Laricchia G 2006 *Nucl. Instrum. Methods Phys.* B **247** 92
[17] Arcidiacono C, Beale J, Pesic Z D, Kover A and Laricchia G 2009 *J. Phys. B: At. Mol. Opt. Phys.* **42** 065205
[18] Hervieux P-A, Fojon O A, Champion C, Rivarola R D and Hanssen J 2006 *J. Phys. B: At. Mol. Opt. Phys.* **39** 409
[19] Baluja K L, Zhang R, Franz J and Tennyson J 2007 *J. Phys. B: At. Mol. Opt. Phys.* **40** 3515

[20] Sullivan J P, Jones A, Caradonna P, Makochekanwa C and Buckman S J 2008 *Rev. Sci. Intrum.* **79** 113105
[21] Murphy T J and Surko C M 1992 *Phys. Rev.* A **46** 5696
[22] Gilbert S J, Kurz C, Greaves R G and Surko C M 1997 *Appl. Phys. Lett.* **70** 1944
[23] Sullivan J P, Gilbert S J, Marler J P, Greaves S J, Buckman S J and Surko C M 2002 *Phys. Rev.* A **66** 042708
[24] Sullivan J P, Makochekanwa C, Jones A, Caradonna P and Buckman S J 2008 *J. Phys. B: At. Mol. Opt. Phys.* **41** 081001
[25] Coolidge A S 1928 *J. Am. Chem. Soc.* **50** 2166
Coolidge A S 1930 *J. Am. Chem. Soc.* **52** 1874
[26] Waring W 1951 *Chem. Rev.* **51** 171
[27] Takaishi T and Sensui Y 1963 *Trans. Faraday Soc.* **59** 2503
[28] Silva H, Muse J, Lopes M C A and Khakoo M A 2008 *Phys. Rev. Lett.* **101** 033201
[29] Vizcaino V, Jelisavcic M, Sullivan J P and Buckman S J 2006 *New J. Phys.* **8** 85
[30] CRC Handbook of Chemistry and Physics 2007–2008 88th edn, ed D R Lide (Cleveland, OH: CRC Press)
[31] Bettega M H F and Lima M A P 2009, private communication
[32] Tennyson J 2009, private communication
[33] Bettega M H F 2006 *Phys. Rev.* A **74** 054701
[34] Gianturco F A, Mukherjee T and Occhigrossi A 2001 *Phys. Rev.* A **64** 032715
[35] Baluja K L and Jain A 1992 *Phys. Rev.* A **45** 7838
[36] De-Heng S, Jin-Feng S, Xiang-Dong Y, Zun-Lue Z and Yu-Fang L 2004 *Chin. Phys. Soc.* **13** 1018
[37] Campeanu R I, Fromme D, Kruse G, McEachran R P, Parcell L A, Raith W, Sinapius G and Stauffer A D 1987 *J. Phys. B: At. Mol. Phys.* **20** 3557
[38] Coleman P G, Cheesman N and Lowry E R 2009 *Phys. Rev. Lett.* **102** 173201
[39] Banković A, Petrović Z Lj, Robson R E, Marler J P, Dujko S and Malović G 2009 *Nucl. Instrum. Methods Phys.* B **267** 350
[40] Marler J P, Petrović Z Lj, Banković A, Dujko S, Šuvakov M, Malović G and Buckman S J 2009 *Phys. Plasmas* **16** 057101
[41] Šuvakov M, Petrović Z Lj, Marler J P, Buckman S J, Robson R E and Malović G 2008 *New J. Phys.* **10** 053034
[42] White R D and Robson R E 2009 *Phys. Rev. Lett.* **102** 230602